Effect of Temperature on the Charpy Impact and CTOD Values of Type 304 Stainless Steel Pipeline for LNG Transmission

Jong-Hyun Baek*, Young-Pyo Kim, Woo-Sik Kim, Young-Tai Kho
R&D Division, Korea Gas Corporation, 638-1 Il Dong, Ansan, Kyunggi-Do 425-790, Korea

Stainless steel pipe of type 304 the with a wall thickness of 26.9 mm and the outer diameter 406.4 mm is welded by manual arc welding process. Mechanical properties and fracture toughness of type 304 stainless steel are investigated in the temperature ranging from room temperature to −162℃. The results obtained are summarized as follows. The tensile strength noticeably increases as the temperature becomes lower while the yield strength is relatively insensitive to temperature. The Charpy impact energy and CTOD values become higher in the case that crack propagation direction is aligned to the transverse axis upon the rolling direction than longitudinal direction. The drop of fracture toughness is associated with the noticeable diminution of plastic component as temperature seduces from room temperature to −162℃.

Key Words : Austenitic Stainless Steel, Tensile Strength, Charpy Impact Energy, CTOD, LNG, Fracture Toughness, SMAW, SAW

1. Introduction

The materials for storage, transmission and vaporization of Liquefied Natural Gas (LNG) should have good mechanical properties at cryogenic temperatures because the boiling point of LNG is −162℃ under 1 atmosphere pressure (Nakamura et al., 1982 ; Tsuzaki et al., 1983). Structural alloys for cryogenic application should exhibit high strength, ductility, fracture toughness, good weldability and good fabrication (Avery et al., 1995 ; Mills, 1997). Austenitic stainless of AISI type 304 is widely used for LNG utilities thanks to its good metallurgical and mechanical properties. The 304 austenitic stainless pipes for LNG transmission are being joined by welding, and the fracture origins of welded structures are mainly from the degradation of mechanical properties due to variation in microstructures resulting from the thermal cycles during welding (Lancaster, 1993). The thermal conductivity of 304 austenitic stainless is one third of that of carbon steel at room temperature and about two thirds of that of carbon steel at temperature over 700℃. On the other hand, the thermal expansion coefficient of 304 austenitic stainless is about one and half higher than that of carbon steel (Gordon et al., 1965). This could incsease distortion, bucking and cracking at the welding joint. There have been many studies on the fracture toughness of the weld metal and base metal of austenitic stainless steel (Read, 1980 ; Matsumoto et al., 1987 ; Nishimura et al., 1998 ; Marshall, 1984). However, little research has been done on the fracture toughness properties at the LNG temperature of −162℃. The tensile and fatigue properties were investigated on the base metal of austenitic stainless steel at temperature between 20℃ and −162℃ (Mukai et al., 1979). The tensile and fracture toughness tests were

* Corresponding Author,
E-mail : jhbaek@kogas.re.kr
TEL : +82-31-400-7487; **FAX** : +82-31-416-9014
R&D Division, Korea Gas Corporation, 638-1 Il Dong, Ansan, Kyunggi-Do 425-790, Korea. (Manuscript **Received** June 13, 2001; **Revised** May 16, 2002)

Table 1 Girth welding condition

Weld processes	Filler metal		Electrical properties			Travel speed (cm/min.)	Heat input (kJ/cm)
	Electrode	Dia.	Polarity	Amp.	Vol.		
GTAW ($1\sim4^{th}$ pass)	ER308L	2.4	DCSP	151~160	17.5~19.6	18.3~36.4	4.3~10.3
SMAW ($5\sim10^{th}$ pass)	E308L	3.2	DCRP	87.4~98.6	30.0~33.2	4.6~8.8	18.0~42.8

performed for the 304 stainless steel plate with the thickness of 2 mm used for membrane type LNG storage tank (Kim et al., 2000). The biaxial fatigue life test of the shaped membrane sheet was evaluated with the temperature change $\Delta T=190℃$ (Kim, 2001). They did not deal with the fracture toughness of the base metal or the mechanical properties of the weld metal. The elastic-plastic fracture mechanics approach to analyze the fracture behavior of the weld metal has become a valuable method in establishing design criteria and structural integrity. The Charpy impact and CTOD tests to evaluate integrity using specimens machined from the welded 304 austenitic stainless pipes over the temperature ranging from room temperature to −162℃ are described and discussed in this paper.

2. Experimental Procedures

The material used in the study is the 304 austenite stainless steel pipe for LNG transmission. This pipe of the wall thickness 26.9 mm and the outer diameter 406.4 mm was welded by a submerged arc welding (SAW) in the longitudinal direction. A seam weld is conducted by the SAW process with the conditions of 400~800 A and 28~40 V, and a travel speed of 30~55 cm/min with a filler metal of ER308L. A girth welding was produced with a compound V-groove level, root gap 2~4 mm and root face 0.8~2.4 mm. The girth welding process was done by gas tungsten arc welding (GTAW) with a filler metal of ER308L up to the 4th pass followed by shielded metal arc welding (SMAW) with an E308L electrode for the remaining passes. Details of the girth welding conditions are given in Table 1. The polished samples were electrolytically etched in a solution of 10cc oxalic acid and 90 cc distilled water. The Charpy V-notch specimens (10×10×55mm) were extracted from

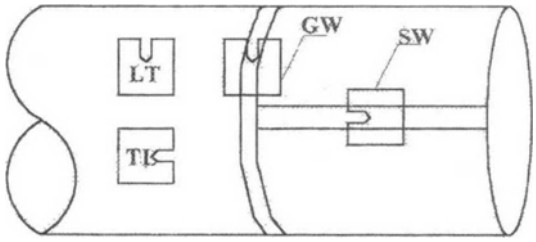

Fig. 1 Schematic illustration of the direction of crack propagation

the T/2 location and notched along the weld centerline in the through-thickness orientation. Figure 1 illustrates the crack orientation of the specimens in the welded pipe. The Charpy impact tests were carried out at three different temperatures in accordance with ASTM standard (ASTM E23-96, 1996). A scanning electron microscope (SEM) was used to examine the morphology of the fractured weld metal. The CTOD tests (BS 7448, 1991) were conducted at each temperature to evaluate the fracture toughness, and those were carried out using the specimens of the B×2B rectangular type of the thickness 13 mm. Testing was carried out at three points bending under displacement control under the crosshead displacement rate of 1 mm/min. Tensile tests according to ASTM E8M were carried out at the same temperature as the CTOD test so that the yield strength results could be included in the CTOD calculations. Weld metal hardness was measured on transverse sections, using a micro Vickers diamond pyramid indenter and a 500 g load. The space between two adjacent testing spots was 1 mm.

3. Results and Discussion

3.1 Chemical composition and microstructure observation

The chemical compositions of the base metal and weld metals are given in Table 2. There are

Table 2 Chemical composition of the base metal and weld metal (wt. %)

Specimens	C	Mn	P	S	Si	Ni	Cr	Mo	Nb	Fe	Creq	Nieq
Base	0.096	1.54	0.04	0.011	0.82	9.56	16.05	0.09	0.02	Bal.	17.37	12.65
Seam	0.076	1.24	0.04	0.016	0.92	8.63	16.68	0.07	0.05	Bal.	18.17	13.14
Girth	0.025	0.74	0.04	0.011	0.79	9.89	16.68	0.09	0.05	Bal.	17.99	13.00

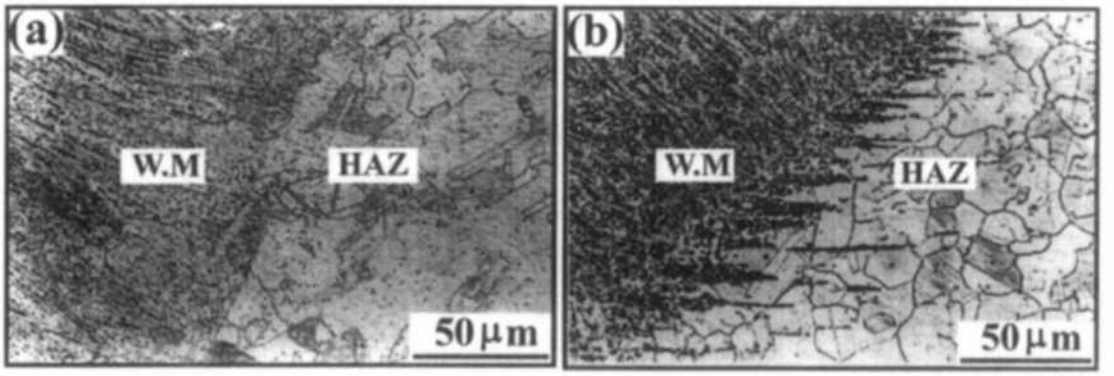

(a) Weld metal/HAZ of seam welds (b) Weld metal/HAZ of girth welds

Fig. 2 Microstructure of the seam and girth weld metal on the Type 304 Stainless steel

small differences in Cr and Ni contents. The carbon content is the highest for the base metal at 0.096%, while the girth weld has the lowest value of 0.025%. Sulphur and phosphorous contents are within the ASTM A312 and AWS SFA 5.4, 5.9 specifications. The Cr_{eq} on the girth weld and seam weld is found, from the calculation, to be 17.99 and 18.17 respectively, while Ni_{eq} is 13.00 and 13.14, respectively. And, Cr and Ni equivalents are calculated from Cr_{eq}= %Cr+%Mo+1.5×%Si+0.5×%Nb and Ni_{eq}= %Ni+30×%C+0.5X%Mn. Microstructures of the seam and girth weld metal are shown in Fig. 2. Figure 2(a) indicates the boundary of weld metal and heat-affected zone (HAZ) in the seam weld that is not observed sensitization due to the welding thermal cycles. The pipe used in present work was welded by means of the SAW process which was underwent a post weld heat treatment (PWHT) at 1050℃ for 30 min followed by water quenching. The PWHT was conducted to remove the sensitization phenomenon and the loss of corrosion resistance due to diffusion of the grain boundary of chromium (Jones, 1992). Figure 2(b) presents the boundary of the weld metal and the HAZ in the girth weld. The grain boundary and bond zone were sensitized as a result of the welding thermal cycles. The sensitization at the grain boundary and bond zone was not eliminated because the PWHT was not conducted for the girth welds. When the stainless steel pipe is exposed for long period of time in the temperature range of 430~870℃, carbon in the steel forms chromium-carbides with the chromium. These carbides are formed preferentially at the grain boundary, and thus the boundary becomes depleted of chromium. The lower chromium levels are resulted from the loss of corrosion resistance (Ikawa, 1972). The pipe for LNG transmission would require good mechanical properties and toughness rather than corrosion resistance at cryogenics temperatures. We think that the sensitization in the micro size region such as the HAZ does not matter for the safe transmission of LNG.

3.2 Micro-hardness and tensile properties

The results of hardness distribution on the weld metals are given in Fig. 3. The hardness distributions in the seam weld metal are in the range of 150~210 Hv at the top of the weld and 175~239 Hv at the root of the weld. In the case

of the girth weld metal, the hardness variation changes from 221~283 Hv at the top bead to 200~248 Hv at the root of the weld metal. The seam weld metal has a lower hardness than the girth weld metal due to the effect of stress relieving by the PWHT. Figure 4 indicates the effect of the temperature on the tensile strength and the yield strength properties. The yield strength was measured by the 0.2% offset method. The yield strength of the longitudinal and transverse axes upon the rolling direction of the base metal is 288 MPa and 297 MPa at the room temperature. The yield strengths of 354 MPa and 373 MPa are observed at −162℃. The yield strength of weld metals has a similar tendency like the base metal. In all specimens tested, the tensile strength at −162℃ is about twice as high as the tensile strength at room temperature. In Fig. 4, the tensile strength of the base and weld metal noticeably increase as the temperature goes lower, while the variation in yield strength are relatively insensitive to temperature. Previous investigators observed the increase of tensile strength with temperature decrease and this increase was associated with the formation of strain-induced martensite during deformation (Mukai, 1972; Huang, 1989).

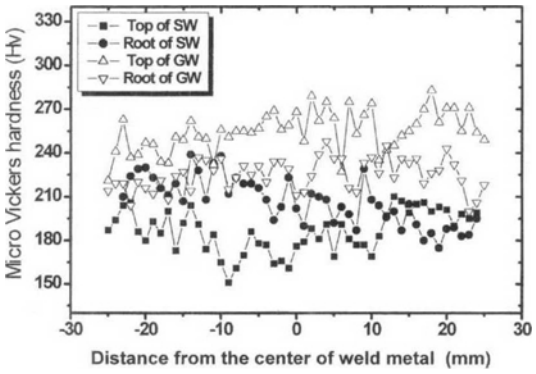

Fig. 3 Hardness distribution of the weld metals

3.3 Charpy impact tests

The results of the Charpy impact values are shown in Fig. 5 against the temperature change. In the base metal, the Charpy impact produces higher value than 120 J even at −196℃. From Fig. 5, the Charpy impact property is affected by the notch orientation upon the rolling direction of base metal. The Charpy impact energy shows a higher value when the crack propagation direction is aligned to the transverse axis, upon the rolling direction, than longitudinal direction. The Charpy impact values on the seam and girth weld metal are 44.2 and 31.4 J, respectively, when the test temperature is −196℃. Figure 6 presents the scanning electron microphotography of the base and weld metals at −196℃. All specimens failed by a dimple fracture at the tested temperature. The inclusions of spherical morphology were examined in the dimples of the weld metal Figs. 6(c) and 6(d). Examples of energy dispersive X-ray analysis on the inclusions of Fig. 6(c) and 6(d) are shown in Fig. 6(e) and 6(f). It is found from EDS measurement that the inclusions investigated in this work are pre-

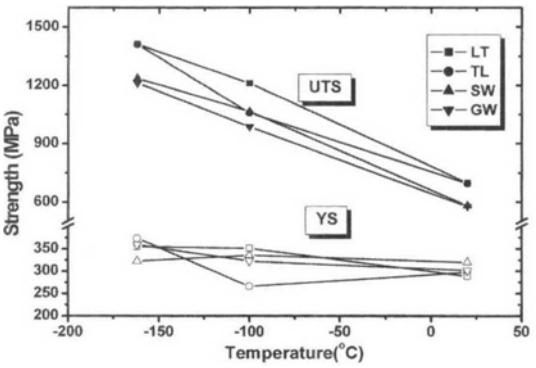

Fig. 4 Strength properties of the base metal and weld metals

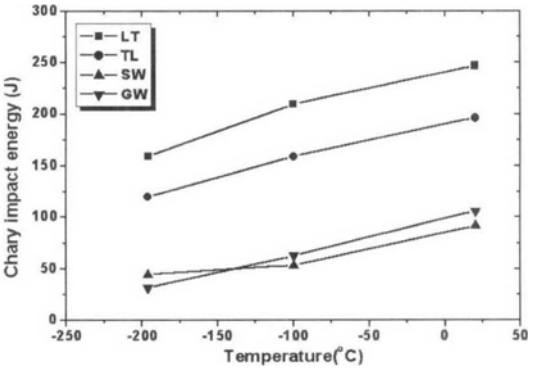

Fig. 5 Charpy impact energy of the base metal and weld metals

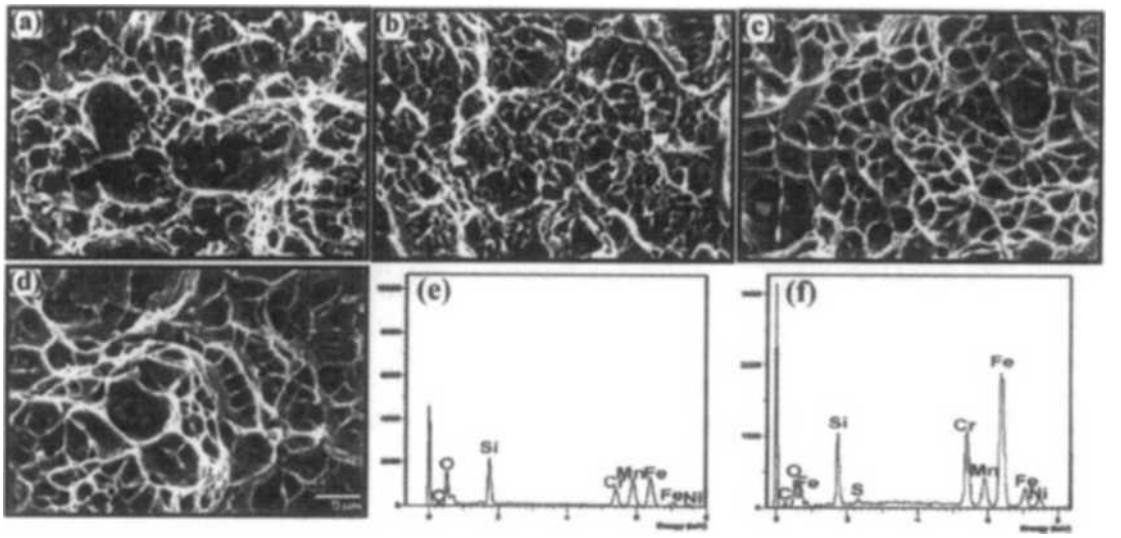

Fig. 6 SEM photographs and EDS of the base and weld metal on the Charpy impact specimens at −196℃ : (a) LT of BM, (b) TL of BM, (c) SW, (d) GW, (e) EDS of Fig. 6(c), (f) EDS of Fig. 6(d)

dominantly type of complex of oxides and sulfide which usually consist of silicon and manganese.

3.4 CTOD tests

The test was based on BS 7448, and CTOD values were calculated from Eqs. (1) and (2).

$$\delta=\left[\frac{FS}{BW^{1.5}}\times f\left(\frac{a_o}{W}\right)\right]^2\frac{1-\nu^2}{2\sigma_{YS}E}+\frac{0.4(W-a_o)V_P}{0.4W+0.6a_o+z} \quad (1)$$

$$f\left(\frac{a}{W}\right)=\frac{3\left(\frac{a_o}{W}\right)^{0.5}\left[1.99-\left(\frac{a_o}{W}\right)\left(1-\frac{a_o}{W}\right)\left(2.15-\frac{3.93a_o}{W}+\frac{2.7a_o^2}{W^2}\right)\right]}{2\left(1+\frac{2a_o}{W}\right)\left(1-\frac{a_o}{W}\right)^{1.5}} \quad (2)$$

Where, F is the applied force, S the distance between outer loading points in the three point bend test, W the specimen width, B the specimen thickness, a_o the average original crack length, ν the Poisson's ratio, E the Young's modulus of elasticity, σ_{YS} 0.2% proof strength, V_P the plastic component of notch opening displacement near mouth, and z the distance of the notch opening gauge location above the surface of the specimen. The CTOD values were calculated at maximum load, and there was no pop-in and unstable crack propagation during the tests. The CTOD approach is the most widely applied method in the elastic plastic fracture mechanics analysis of welded structures (Harrison, 1980). The CTOD value in Eq. (1) is expressed in terms of the summation of the elastic and plastic components (*i.e.* $\delta=\delta_{\text{elastic}}+\delta_{\text{plastic}}$). Figure 7 shows the CTOD values as elastic and plastic terms. The elastic and plastic components have range of 0.026~0.05 mm and 0.357~2.054 mm, respectively. The plastic components noticeably decrease as the temperature becomes lower, while the elastic components are relatively insensitive to temperature. The decrease in fracture toughness of the material used in the study is associated with the steep diminution of the plastic component as the temperature goes lower from room temperature to −162℃. The elastic component of the TL specimen at −100℃ shows higher value compared to other specimens. It is related to the yield strength of the TL specimen at −100℃ from the Fig. 4. The elastic part of the CTOD value is in the reciprocal proportion relation with the yield strength, according to the first component on the right-hand in Eq. (1). Figure 8 indicates fractographs of CTOD specimens of the base and weld metals. Formed dimples in the transverse direction are much deeper and larger than those in the longitudinal axis upon the rolling direction. It is because the development of the crack front is hindered by the grain boundary when the crack propagates to the transverse of the rolling

direction during CTOD tests. Also there is an obvious difference in the size of dimple on the base metal depending on the temperature. The dimple size decreases from 10~15 μm (not presented here) to 3~4 μm [Fig. 8(a), (b)] as the temperature drops from room temperature to −162℃. But the effect of temperature has a little influence on the weld metals. From the size and depth of dimples, we presume that there is an improvement of fracture toughness in the base metal when compared to the weld metal. There is also a clear difference in the magnitude and depth of the dimples and in the CTOD values between room temperature and −162℃, from a result of CTOD tests on the base metal. Therefore, the difference of the CTOD values and size of dimples to a variation of temperature is associated with some extent of micro-void coalescence in the metal during CTOD tests. A spherical inclusion with a size of 1~2 μm is examined in the dimples at the weld metal Figs. 8(c) and 8(d). Examples of energy dispersive X-ray analysis on the inclusions of Figs. 8(c) and 8(d) are shown in Figs. 8(e) and 8(f). These inclusions were determined as a compound consisting of silicon, manganese, oxygen and sulphur. In general, silicon inclusion in weld metal has a detrimental influence on the fracture resistance (Mills, 1997) So, the interface between the inclusions consisted of silicon compound and the matrix is easily separated at the low plastic deformation that caused decreasing of CTOD values.

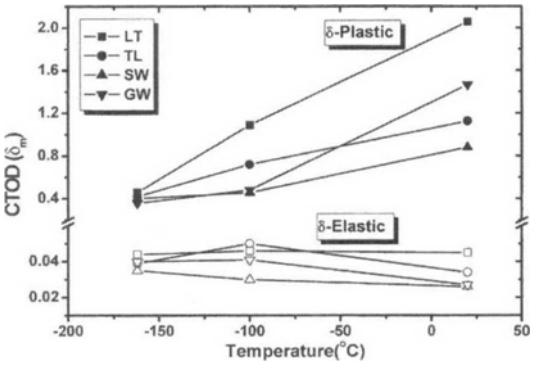

Fig. 7 CTOD values of the base metal and weld metals

4. Conclusions

The Charpy impact and CTOD tests for type 304 stainless steel and weld metal were studied over the temperature range from room temperature to −162℃.

(1) The tensile strength noticeably increases as the temperature goes lower while the yield strength is relatively insensitive to temperature.

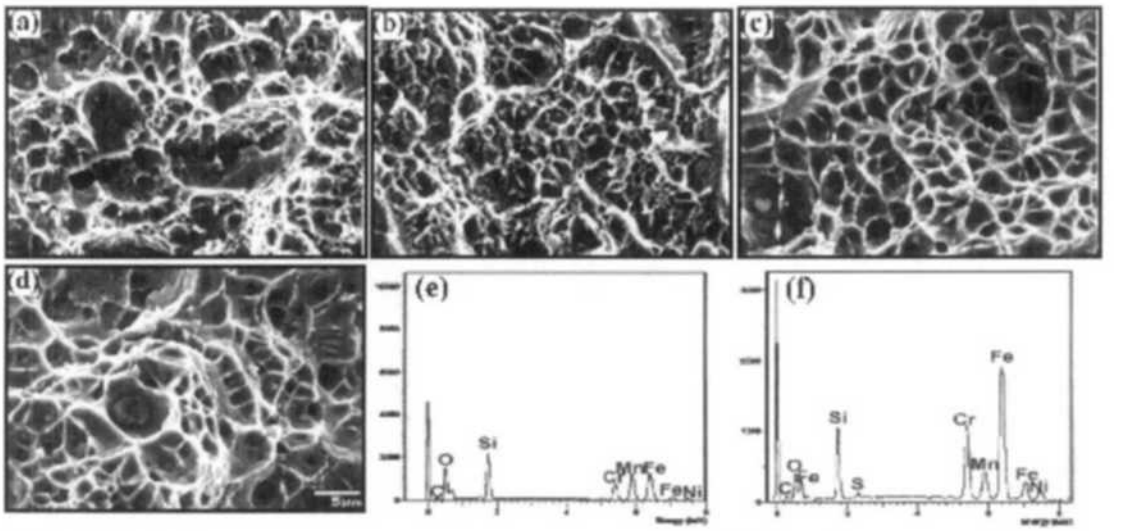

Fig. 8 SEM photographs and EDS of the base and weld metal on the CTOD specimens at −162℃ : (a) LT of BM, (b) TL of BM, (c) SW, (d) GW, (e) EDS of Fig. 8(c), (f) EDS of Fig. 8(d)

The increment of the tensile strength in plastic deformation range is associated with the formation of strain-induced martensite during deformation.

(2) The Charpy impact energy and CTOD values show higher value in the case of crack propagation direction is aligned to the transverse axis, upon the rolling direction, than longitudinal direction because the development of the crack front is hindered by the grain boundary.

(3) The drop of fracture toughness is associated with the noticeabe diminution of plastic component as temperature decreases from room temperature to −162℃.

(4) The interface between the inclusions consisted of silicon compound and the matrix is easily separated at the low plastic deformation that caused by the decrease in the Charpy impact energy and CTOD values.

References

Avery, R. E. and Parsons, D., 1995, "Welding Stainless and 9% Nickel Steel Cryogenic Vessels," *Weld. J.*, Vol. 74, No. 11, pp. 45~50.

ASTM E 23-96, 1996, "Standard Test Methods for Notched Bar Impact Testing of Metallic Materials," *Annual Book of ASTM Standards*, Vol. 03.01.

BS 7448, 1991, "Part 1. Method for Determination of K_{IC}, Critical CTOD and Critical J Values of Metallic Materials," *British Standards*.

Gordon, J. and Hanson, A., 1965, *An Introduction to Stainless Steel*, ASM, Metals Park, OH, pp. 137~138.

Harrison, J. D., 1980, "The 'State-of-the-Art' in Crack Tip Opening Displacement (CTOD) Testing and Analysis," *Metal Construction*, Vol. 12, No. 9, pp. 415~422.

Huang, G. L., Matlock, D. K. and Krauss, G., 1989, "Martensite Formation, Strain Rate Sensitivity and Deformation Behavior of Type 304 Stainless Steel Sheet," *Metall. Trans. A*, Vol. 20A, No. 7, pp. 1239~1246.

Ikawa, H., 1972, "Welding Metallurgy of Austenitic Stainless Steel," *Journal of the Japan Welding Society*, Vol. 41, No. 2, pp. 9~20.

Jones, D. A., 1992, *Principles and Prevention of Corrosion*, Macmillian Publishing Co., New York, pp. 291~293.

Kim, C. S., Kim, J. K., Cho, D. H., Yoon, I. S. and Kim, D. S., 2000, "Low Temperature Effects on the Strength and Fracture Toughness of Membrane Material for LNG Storage Tank," *Transactions of KSME*, Vol. 24A, No. 3, pp. 710~717.

Kim, H. S., 2001, "The Evaluation of Mechanical Properties and Fatigue Life for Domestic 304 Stainless Steel Used as Membrane Material in LNG Storage Tank," *Transactions of KSME*, Vol. 25A, No. 10, pp. 1644~1650.

Lancaster, J. F., 1993, *Metallurgy of Welding*, Chapman & Hall, London, UK, pp. 152~162, 5th ed.

Marshall, A., 1984, "Effects of Residual, Impurity and Microalloying Elements on Properties of Austenitic Stainless Steel Weld Metals." *Metal Construction*, Vol. 16, No. 6, pp. 347~352.

Matsumoto, T., Satoh, H., Wadayama, Y. and Hataya, F., 1987, "Mechanical Properties of Fully Austenitic Weld Deposits for Cryogenic Structures," *Weld. J.*, Vol. 66, No. 4, pp. 120-s~126-s.

Mills, W. J., 1997, "Fracture Toughness of Type 304 and 316 Stainless Steels and Their Welds," *International Materials Reviews*, Vol. 42, No. 2, pp. 45~82.

Mukai, K., Hoshino, K. and Fujioka, T., 1979, "Tensile and Fatigue Properties of Austenitic Stainless Steels at LNG Temperature," *Tetsu-to-Hagane*, Vol. 65, No. 12, pp. 1756~1765.

Nakamura, T., Tominaga, M., Murase, H. and Nishiyama, Y., 1982, "Low Cycle Fatigue Behavior of Austenitic Stainless Steel at Cryogenic Temperature," *Tetsu-to-Hagane*, Vol. 68, pp. 471~476.

Nishimura, A., Tobler, R. L., Tamura, H., Imagawa, S. and Yamamoto, J., 1998, "Fracture Toughness of Thick-section Weld Joint of SUS 316 at Cryogenic Temperature," Fusion Engineering and Design. Vol. 42, pp. 425~430.

Read, D. T., Mchenry, H. I., Steinmeyer, P. A. and Thomas, R. d., 1980, "Metallurgical and Nitrogen in Stainless Steel SMA Welds for

Cryogenic Service," Weld. J., Vol. 59, No. 4, pp. 104-s~113-s.

Tsuzaki, K., Nakanishi, E., Maki, T. and Tamura, I., 1983, "Low Cycle Fatigue Behavior in Metastable Austenitic Steel Accompanying Deformation-Induced Martensitic Transforation," ISIJ, Vol. 23, pp. 834~841.